Journal of Alloys and Compounds, 187 (1992) 49–57
JALCOM 309

Microstructures and hydrogenation properties of $TiFe_{1-x}M_x$ alloys

S.-M. Lee and T.-P. Perng*
Department of Materials Science and Engineering, and Materials Science Center, National Tsing Hua University, Hsinchu (Taiwan)

H.-K. Juang, S.-Y. Chen, W.-Y. Chen and S.-E. Hsu
Materials Research and Development Center, Chung Shan Institute of Science and Technology, Lung-Tan, Tao-Yuan (Taiwan)

(Received February 10, 1992)

Abstract

The hydrogen absorption characteristics of TiFe partially substituted with a small amount of chromium or manganese for iron were studied. The morphology of the specimen surface was examined and the phases in the sample were identified. The microscopic composition differences for the individual phases were analysed. It was observed that the samples required no activation for hydrogenation when a second phase was present. Increasing the amount of second phase led to a higher activation rate, lower plateau pressure and higher maximum absorption capacity. Homogenization treatment at 900 °C reduced the activation rate but had no effect on the subsequent hydrogenation properties. The effects of substitution and homogenization on the hydrogenation of TiFe were correlated with the quantity and morphology of the second phase.

1. Introduction

TiFe is one of the most effective materials for hydrogen storage [1]. However, the virgin compound reacts very slowly with hydrogen at room temperature even at high hydrogen pressures. A high temperature heat treatment is required in order to activate the sample to absorb hydrogen at room temperature. Furthermore, the reversible transfer capacity of hydrogen of TiFe decreases significantly after repeated hydrogenation and dehydrogenation in the presence of other gases in hydrogen.

To overcome the above disadvantages, it has been proposed that iron in TiFe be substituted by a third element such as aluminium, manganese, nickel, chromium or sulphur [2–10]. For instance, when a small amount of manganese is substituted for iron, the activation is promoted and the resistance to impure gases is also enhanced [11]. Although the effects of this substitution have been widely reported, the reasoning behind the effects is still not well understood. Yang *et al.* [7] proposed that, when $TiFe_{0.9}Mn_{0.1}$ was heated to 100 °C in a vacuum, surface aggregation of manganese took place and

*Author to whom correspondence should be addressed.

0925-8388/92/$5.00

$TiMn_{1-2}$ was formed. $TiMn_{1-2}$ was first hydrogenated and served as a window of the matrix to absorb hydrogen, thus promoting the activation of $TiFe_{0.9}Mn_{0.1}$. A similar mechanism of activation of TiFe based upon the formation and/or addition of a second phase has also been reported by Zhang *et al.* [12]. It is therefore desirable to study the changes in hydrogenation properties of TiFe due to these alloying elements in more detail and to correlate the properties with the addition of the elements and the second phases.

In this paper, the metallurgical structures and the activation as well as some other hydrogen absorption characteristics of Ti–Fe–Mn and Ti–Fe–Cr ternary alloys are studied. The mechanism of activation is discussed on the basis of structural features of the alloys. The effect of homogenization on hydrogen absorption properties is also examined.

2. Experimental details

The raw materials used were iron (purity, 99.9 wt.%), chromium (purity, 99.6 wt.%), manganese (purity, 99.9 wt.%) and titanium (purity, 99.5 wt.%). Four compounds $TiFe_{0.9}Mn_{0.1}$, $TiFe_{0.8}Mn_{0.2}$, $TiFe_{0.95}Cr_{0.05}$ and $TiFe_{0.9}Cr_{0.1}$ were prepared in an arc furnace under an argon atmosphere. The ingots were turned and remelted five times during the arc melting in order to homogenize the specimens. Some of these samples were further annealed (*i.e.* homogenization treatment) at 900 °C in vacuum for 80 h to eliminate segregation.

All the samples were crushed in an ambient atmosphere and only powders of mesh size from +20 to −50 were selected for the hydrogenation experiments. The hydriding rate and pressure–composition isotherms were measured using a conventional high pressure volumetric system [13]. For each run, approximately 7 g of alloy powder were loaded in the reactor which was sealed and evacuated. Hydrogen gas at 4.0 kgf cm^{-2} was then introduced into the reactor. The pressure change of hydrogen was recorded as a function of time. The pressure–composition isotherms for hydrogen absorption and desorption were obtained by adding or withdrawing a known amount of hydrogen from the reaction system.

The microstructures of the sample powders before and after hydrogenation were investigated by optical metallography and scanning electron microscopy (SEM). The phases were identified by powder X-ray diffraction (XRD).

3. Results and discussion

The XRD patterns for the as-melted samples are shown in Fig. 1. For both $TiFe_{0.95}Cr_{0.05}$ and $TiFe_{0.9}Cr_{0.1}$, the XRD patterns showed that some $TiCr_2$ was present besides the TiFe phase. The amount of $TiCr_2$ increased with increasing amount of chromium in the alloy. For $TiFe_{0.8}Mn_{0.2}$, some $TiMn_{1.5}$ (η phase) was observed, whereas $TiFe_{0.9}Mn_{0.1}$ exhibited a single-phase pattern. Annealing of the samples did not change the features of the XRD patterns.

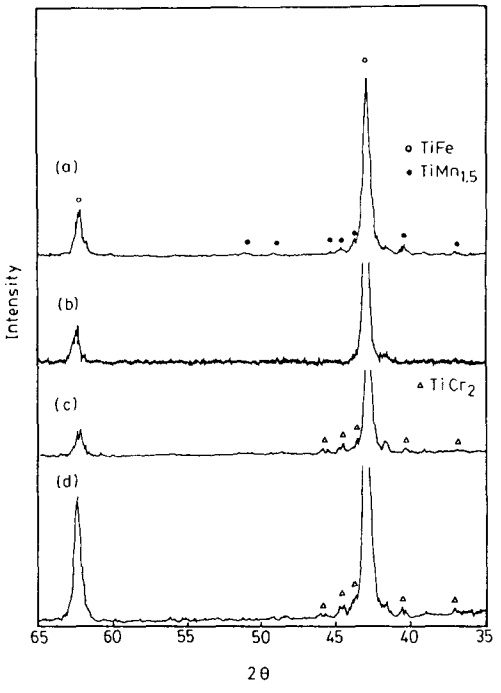

Fig. 1. XRD patterns for as-melted samples: (a) $TiFe_{0.8}Mn_{0.2}$; (b) $TiFe_{0.9}Mn_{0.1}$; (c) $TiFe_{0.9}Cr_{0.1}$; (d) $TiFe_{0.95}Cr_{0.05}$.

The rates of hydrogen absorption for the two alloys $TiFe_{0.95}Cr_{0.05}$ and $TiFe_{0.9}Cr_{0.1}$ under an initial hydrogen pressure of 40 kgf cm^{-2} in the first hydrogenation cycle at room temperature are shown in Fig. 2. The hydrogen content in each alloy is normalized with respect to the saturated hydrogen content. After a short period of incubation, all specimens started to absorb hydrogen. The incubation time decreased as the amount of chromium increased, and annealing of the specimens led to a longer incubation time. The absorption rate was strongly dependent on the chromium content and heat treatment. $TiFe_{0.9}Cr_{0.1}$ in the as-melted condition had the highest rate, while $TiFe_{0.95}Cr_{0.05}$ after annealing had the lowest rate.

Similar features were also observed for the manganese-substituted compounds. The hydrogenation curves for $TiFe_{1-x}Mn_x$ are shown in Fig. 3. Note that $TiFe_{0.9}Mn_{0.1}$, which was a single-phase material on examination by XRD, could also absorb hydrogen without activation, although the absorption rates were far lower than those of $TiFe_{0.8}Mn_{0.2}$. The incubation time of this sample was about 2 h and it took more than 2 days to reach the saturated value. Annealing slowed down rather than improved the hydrogenation rate.

Micrographs of $TiFe_{0.95}Cr_{0.05}$ and $TiFe_{0.8}Mn_{0.2}$ are shown in Figs. 4 and 5 respectively. A dendritic structure was observed for the as-melted specimens, indicating a serious segregation of compositions and phases. Annealing reduced the segregation and the dendrites almost disappeared. Energy-dispersive X-ray analysis showed that the dark strips were chromium or manganese rich.

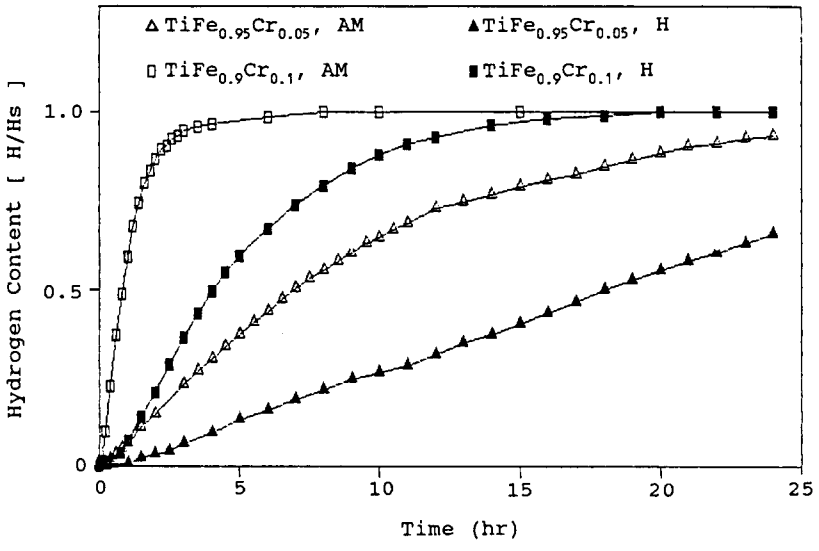

Fig. 2. Hydrogen absorption curves for the first cycle for $TiFe_{1-x}Cr_x$ alloys at room temperature and a hydrogen gas pressure of 40 kgf cm^{-2}: AM, as melted; H, homogenized.

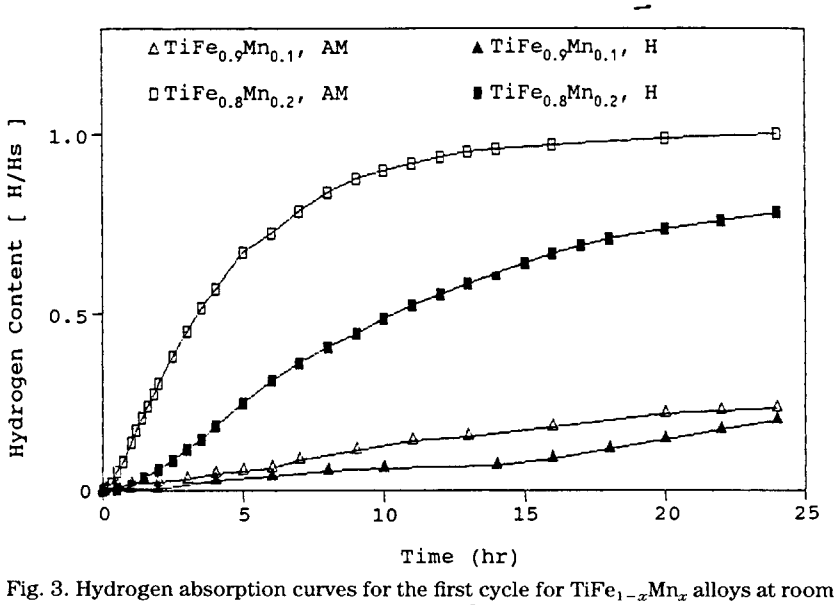

Fig. 3. Hydrogen absorption curves for the first cycle for $TiFe_{1-x}Mn_x$ alloys at room temperature and a hydrogen gas pressure of 40 kgf cm^{-2}.

From the above results, it is seen that the second phase might have affected the activation rates of the $TiFe_{1-x}M_x$ alloys. The changes in the amount and morphology of the second phase after the homogenization treatment were closely related to the hydrogenation behaviour of the compounds. There may be two reasons why the second phase could affect the rate of activation.

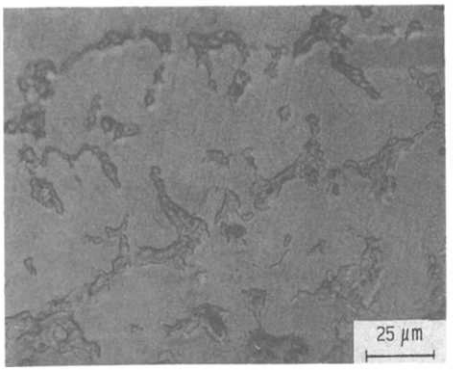

(a)

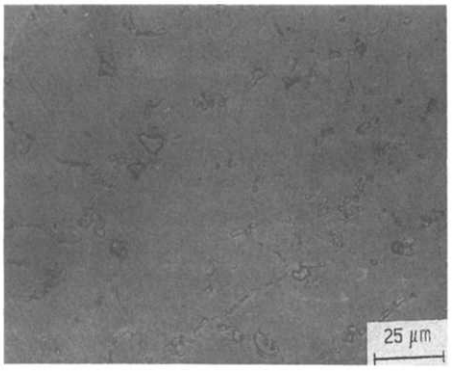

(b)

Fig. 4. Micrographs of the $TiFe_{0.95}Cr_{0.05}$ alloy: (a) as melted; (b) homogenized.

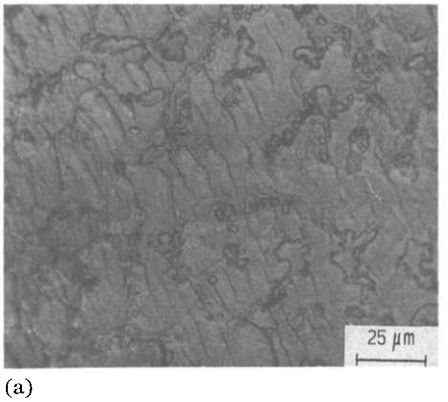

(a)

(b)

Fig. 5. Micrographs of the $TiFe_{0.8}Mn_{0.2}$ alloy: (a) as melted; (b) homogenized.

(1) The second phase is dispersed along the grain boundary of the TiFe matrix; hydrogen reacts more easily with the interface of the two phases, which also provides a preferred path for hydrogen penetration into TiFe. The interfacial region was much larger when dendritic structures were present in the sample. After annealing, the second phase became more spheroidized. The number of paths for hydrogen to diffuse into the alloy decreased as the interfacial region decreased. This resulted in a reduction in activation rate.

(2) The volume of the second phase expands during hydrogenation. The second phases can absorb hydrogen readily to form hydride or solid solution prior to hydrogenation of the TiFe phase in the alloy. The increases in volume of $TiMn_{1.5}$ and $TiCr_2$ after hydrogenation could increase to 27.1% and 17.8% respectively [14, 15]. The stress-induced cracks at the grain boundaries of TiFe might produce a large amount of clean surface of TiFe for hydrogen absorption without activation treatment.

It is conceivable that, if the amount of the second phase is too little, the above two effects become less effective. This was the reason why it

made almost no difference in hydrogenation rate whether $TiFe_{0.9}Mn_{0.1}$ was tested in the as-melted or in the annealed condition.

Figure 6 shows the SEM micrographs of $TiFe_{0.95}Cr_{0.05}$ and $TiFe_{0.8}Mn_{0.2}$, both without homogenization treatment, before and after hydrogenation. It is seen that, after hydrogenation, not only large cracks but also some finer cracks exist. When the micrographs for samples before and after hydrogenation are compared, the regions surrounded by the large cracks have the same shape and size as the virgin grains. This implies that the hydride of second phase was formed prior to the hydrogenation of the TiFe phase and induced the cracking.

The change in volume of pure TiFe after the hydrogenation was only about 4%, which was far smaller than those for $TiMn_{1.5}$ (27.1%) and $TiCr_2$ (17.8%). When the large cracks had been induced by the formation of a second-phase hydride, new fresh surfaces were generated in the TiFe matrix. These surfaces enabled TiFe to react with hydrogen gas directly and additional

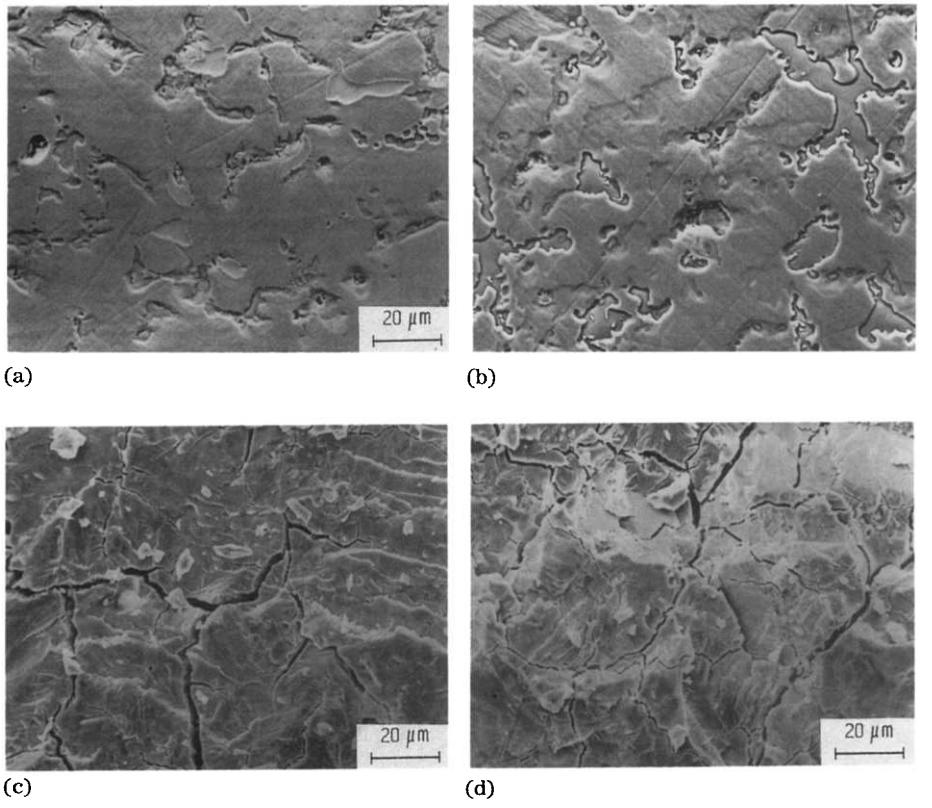

(a) (b)

(c) (d)

Fig. 6. SEM micrographs of as-melted samples: (a) $TiFe_{0.95}Cr_{0.05}$, etched, before hydrogenation; (b) $TiFe_{0.8}Mn_{0.2}$, etched, before hydrogenation; (c) $TiFe_{0.95}Cr_{0.05}$, after hydrogenation; (d) $TiFe_{0.8}Mn_{0.2}$, after hydrogenation.

finer cracks in the TiFe matrix were produced. A similar mechanism has been proposed for $Ti_{1+x}Fe$ compounds previously [13].

The rates of hydrogen absorption for all samples, as melted or annealed, in the second cycle of hydrogenation were very fast. The saturated contents were reached in 10 min, as shown in Fig. 7. Therefore the substitution of iron by a small amount of chromium or manganese could accelerate the activation without losing the hydrogenation kinetics in the subsequent cycles.

Figure 8 shows the pressure–composition curves of the alloys without homogenization. The curve for pure TiFe is also included for comparison. It is seen that the equilibrium pressures in the plateau region for the ternary alloys are all smaller than that of TiFe. In addition, the slopes of the plateaux are higher, while the $TiFeH_2$ regions tend to disappear. The addition of manganese and chromium also increases the maximum absorption capacity of hydrogen in the alloys. Similar curves were obtained for the alloys after the homogenization treatment, as seen in Fig. 9. The homogenization treatment appeared to affect only the hydrogenation kinetics of the first cycle. Once the alloys had started to react with hydrogen, the kinetics and capacities of hydrogenation became an intrinsic property of the alloys.

From this point of view, there is no advantage for $TiFe_{1-x}M_x$ alloys to undergo a homogenization treatment. It is suggested that a small amount of manganese or chromium be substituted for iron in TiFe to accelerate the activation process, and that the alloys be used in as-melted condition to give the best performance of hydrogen storage.

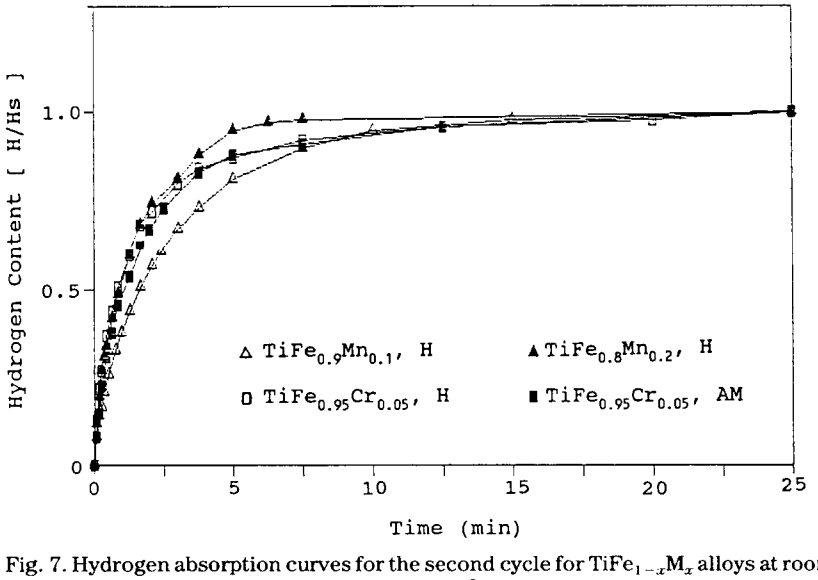

Fig. 7. Hydrogen absorption curves for the second cycle for $TiFe_{1-x}M_x$ alloys at room temperature and a hydrogen gas pressure of 40 kgf cm^{-2}.

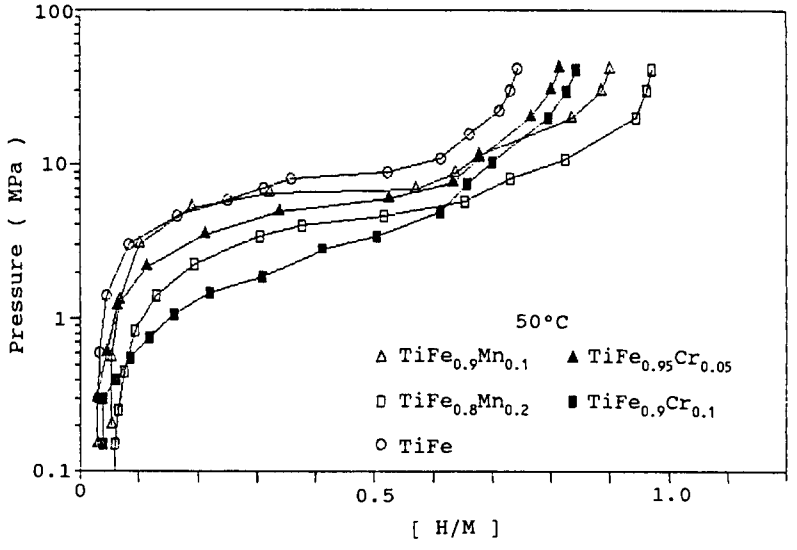

Fig. 8. The dissociation pressure–composition curves for as-melted $TiFe_{1-x}M_x$ at 50 °C.

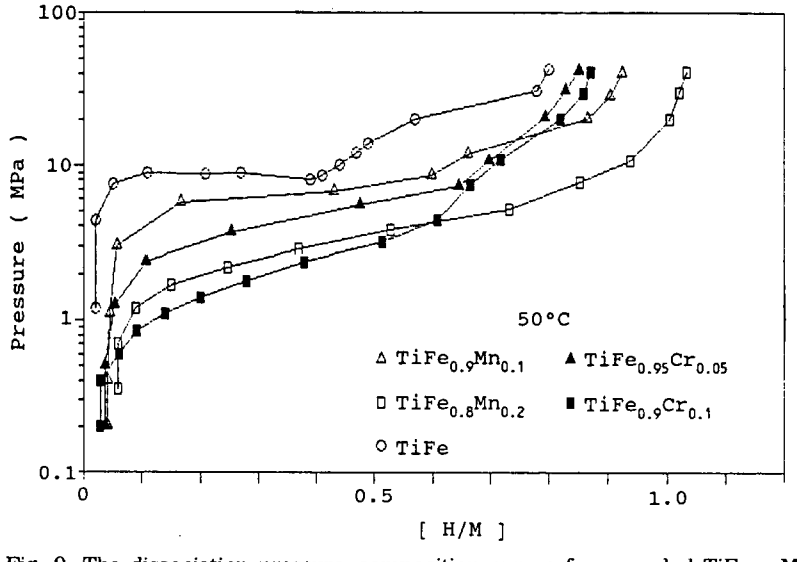

Fig. 9. The dissociation pressure–composition curves for annealed $TiFe_{1-x}M_x$ at 50 °C.

4. Conclusions

The activation of the TiFe compound could be accelerated by substituting a small amount of chromium or manganese for iron without losing the hydrogen absorption capacity. Increasing the amount of chromium and manganese increased the amount of the second phase, and the effect became more pronounced. Homogenization treatment was deleterious to the activation.

The TiFeH region in the pressure–composition curve became more stable and the $TiFeH_2$ region was reduced because of the substitution.

Acknowledgments

This work was supported by the National Science Council of the Republic of China under Contract NSC 79-0405-E-007-24 and Chung Shan Institute of Science and Technology under Contract CS80-0210-D007-05.

References

1 J. J. Reilly and R. H. Wiswall, Jr., *Inorg. Chem.*, *13* (1974) 218.
2 G. Bruzzone, G. Costa, M. Ferretti and G. L. Olcese, *Int. J. Hydrogen Energy*, *6* (1981) 181.
3 S. H. Lim and J.-Y. Lee, *J. Less-Common Met.*, *97* (1984) 59.
4 S. H. Lim and J.-Y. Lee, *J. Less-Common Met.*, *97* (1984) 65.
5 D. Dew-Hughes, *Metall. Trans. A*, *11A* (1980) 1219.
6 T. Schober and C. Dieker, *J. Less-Common Met.*, *104* (1984) 191.
7 S. Yang, R. Ye, T. Huang, S. Zhao and B. Chen, *Int. J. Hydrogen Energy*, *13* (1988) 433.
8 H. S. Chung and J.-Y. Lee, *Int. J. Hydrogen Energy*, *11* (1986) 335.
9 M. H. Mintz, S. Vaknin, S. Biderman and Z. Hadari, *J. Appl. Phys.*, *52* (1981) 463.
10 R. Suzuki, J. Ohno and H. Gondoh, *J. Less-Common Met.*, *104* (1984) 199.
11 G. D. Sandrock and P. D. Goodell, *J. Less-Common Met.*, *73* (1980) 161.
12 Zhang Huiyou, Chen Jianyin, Ping Xinyi and Jiang Jing, in T. N. Veziroglu and P. K. Takahashi (eds.), *Hydrogen Energy Progress VIII, Proc. 8th World Hydrogen Energy Conf., Hawaii, July 1990*, Pergamon Press, 1990, p. 1015.
13 S.-M. Lee and T.-P. Perng, *J. Alloys Comp.*, *177* (1991) 107.
14 R. Hempelmann and G. Hilscher, *J. Less-Common Met.*, *74* (1980) 103.
15 J. R. Johnson, *J. Less-Common Met.*, *73* (1980) 345.